Available online at sjuoz.uoz.edu.krd

Science Journal of University of Zakho
Vol. 12, No. 1, pp. 50 – 56 January-March, 2024

p-ISSN: 2410-7549
e-ISSN: 2414-6943

EFFICIENT SYNTHESIS OF ZNO AS AN ELECTRODE OF PIEZOELECTRIC NANOGENERATORS

Ribar Ameen Salh [a], Mohammed Aziz Ibrahem [a*]
a Department of Physics, College of Science, University of Duhok, Kurdistan Region, Iraq

Received: 16 Sep., 2023 / Accepted: 27 Nov., 2023 / Published: 4 Feb. 2024 https://doi.org/10.25271/sjuoz.2024.12.1.1205

ABSTRACT:

Piezoelectric nanogenerators (NGs) hold immense promise as self-powered devices for harvesting mechanical energy from the environment. This study introduces an efficient and scalable synthesis method for zinc oxide (ZnO) nanorods, a pivotal material in piezoelectric nanogenerators (NGs), with several key results. A Chemical Bath Deposition technique is employed, optimizing parameters such as growth time, temperature, and precursor concentrations to achieve well-aligned and high-quality ZnO nanorods. The structural and morphological characteristics of the synthesized nanorods are systematically investigated using advanced characterization techniques. The synthesized ZnO nanorods exhibit an average length of 400nm, demonstrating their slender shape. Furthermore, the study determines an energy gap value of 3.5 eV for multilayer zinc oxide thin films, indicating the transition from the valence band to the conduction band. Notably, thermal annealing at 500°C leads to a substantial increase in average output voltage, reaching 1.95 V, a fourfold improvement compared to as-deposited nanopowders. These findings emphasize the efficiency and potential of the proposed synthesis method and underscore its practical applications in enhancing energy harvesting capabilities for sustainable power generation from mechanical sources in piezoelectric NGs.

Keywords: Piezoelectric, Zinc Oxide, Nanorods, Nanogenerators, Chemical Bath Deposition.

1. INTRODUCTION:

Zinc oxide (ZnO), an adept inorganic compound, has captured the intrigue of researchers over the preceding decade. Presently, ZnO finds itself integrated into pigments, paints, serums, creams, and more as an additive and forms composites with rubber, ceramics, and glass. Holding promise as a wide band gap semiconductor, ZnO is poised for deployment across an array of electronic devices, encompassing light-emitting diodes, solar cells, sensors, actuators, energy generators, and optoelectronic apparatuses (Wang, 2004). This diversified utility stems from its economical fabrication, adeptness against high temperatures and radiation, substantial exciton binding energy, antibacterial attributes, effective luminescence, and commendable electromechanical coupling properties (Z. Fan & Lu, 2005).

Consequently, zinc oxide earns the distinction of being a multifunctional substance, attainable through various synthesis routes Kołodziejczak-Radzimska, A., and Jesionowski, T. (2014). Zinc oxide—from synthesis to application: a review (Kołodziejczak-Radzimska & Jesionowski, 2014). These diverse methods yield various ZnO structural configurations, each imbued with distinct physical traits, catering to assorted applications. Various morphologies can be achieved in the growth of ZnO nanostructures, encompassing both simple and intricate forms such as nanoneedles, nanorods, nanosheets, nanohelices, nanobelts, and nanowires (Wang, 2004). Each ZnO nanostructure variant possesses distinct synthesis methodologies, properties, and application domains. Among these, ZnO nanorods stand out as a unique entity, boasting an array of features and applications (Rihtnesberg et al., 2011).

Extensive scrutiny is directed towards ZnO nanorods within the medical sphere due to their potent antibacterial attributes (Amna, 2018; Krithika et al., 2017; Kumar et al., 2013) and capacity to combat cancerous cells (Paino, J. Gonçalves, Souza, & Zucolotto, 2016). Moreover, ZnO has found utility in the biosensors (Rezaei, Foroughi, Beitollahi, Tajik, & Jahani, 2019; Tajik, Beitollahi, & Aflatoonian, 2019; Xie, Xu, & Cao, 2013), serving as an industrial photocatalyst (Shinde, Shinde, Bhosale, & Rajpure, 2011; Wahab, Hwang, Kim, & Shin, 2011), and contributing to diverse biotechnological contexts(Umetsu et al., 2005). Its photovoltaic characteristics have prompted its integration as a primary element in solar cells, aligning with the global drive to advance non-traditional energy sources (Mavundla, Malgas, Motaung, & Iwuoha, 2012; Sharma, Dalal, & Mahajan, 2016). Notably, ZnO-based supercapacitors have recently emerged, showcasing commendable high-performance traits (Subramani & Sathish, 2019). A microgenerator is a device that transforms mechanical force into electrical energy. It can produce electricity for a wide array of applications, encompassing self-sustaining electronic gadgets, energy harvesting systems, and medical equipment.

Microgenerators harness a variety of mechanisms, such as displacement current, external photoelectric impact, internal photovoltaic impact, and the triboelectric effect to create electric power. They can operate autonomously without the need for electrodes and offer the benefits of affordability, lightweight, uncomplicated design, and impressive efficiency. Microgenerators hold the potential to overhaul the domains of energy acquisition and power provision, delivering a sustainable and continuous energy source for diverse devices (Ji et al., 2023). Multiple techniques are available for cultivating ZnO nanorods, including microwave heating(Krishnakumar et al., 2009), electrochemical deposition, and chemical polymerization(Shang, Sun, Zhou, & Guan, 2007). A recent focus lies on synthesizing ZnO nanorods with exceptional traits and applications via the hydrothermal route, utilizing zinc acetate dehydrate and N, N-dimethylformamide as precursor substances (J. Fan, Li, & Heng, 2014, 2016).

Furthermore, by diversifying their utility, ZnO nanorods can be grown on varied substrates and combined with other materials to enhance their aptitude, aligning with specific application

* Corresponding author

requisites (Aziz et al., 2014; Yang, Yu, Song, Zhou, & Yao, 2016). Beyond its array of significant attributes, ZnO possesses a notably elevated piezoelectric coefficient. The exertion of force prompts the disjunction of Zn^{2+} and O^{2-} ions, which subsequently accumulate on opposing surfaces, imparting polarization to these surfaces. Efficient collection of these amassed charges facilitates the measurement, storage, and utilization of resulting potential differences or induced currents across a broad spectrum of applications.

In this study, ZnO nanorods are cultivated atop pre-seeded glass substrates through a straightforward hydrothermal process. Notably, the hydrothermal approach stands out as exceptionally efficient, obviating the necessity for catalysts and elevated temperatures. This approach further touts the advantages of cost-effectiveness and reduced hazards owing to the employment of economical and safer chemicals. The synthesis employed here is a tailored rendition of the technique adopted by (Öztürk, Kılınç, Taşaltın, & Öztürk, 2012). for the cultivation of highly aligned ZnO nanorods. The optimization of performance metrics for sensing materials hinges substantially upon their structural attributes, fostering their enhancement. The nanostructure formed by ZnO nanorods, as presented in this study, stands as a viable candidate for impactful applications encompassing transistors, optoelectronic apparatuses, and sensors. Through the utilization of the as-grown ZnO nanostructure, a piezoelectric device is constructed by employing aluminum and copper as the two electrode materials.

Zinc oxide has undergone a comprehensive examination for its potential in nanogenerators, devices capable of transforming mechanical energy into electrical power. Several techniques have been investigated in the creation of ZnO nanostructures, encompassing methods such as hydrothermal synthesis and ion implantation. These strategies have been harnessed to produce arrays of ZnO nanorods and ZnO nanosheets with a structure akin to graphene. These structures have showcased exceptional efficiency and power output when integrated into nanogenerators. Exploiting ZnO's piezoelectric attributes within nanogenerators has yielded promising outcomes, with recorded peak values for voltage and current reaching as high as 5 V and 0.010 μA, respectively (Sun, Zheng, Wang, Fan, & Liu, 2021). It is the adaptability of ZnO across diverse applications, combined with its cost-effective synthesis approaches, that positions it as a material of great potential within the domain of nanogenerators (Kaur, Singh, & Singh, 2020).

Noteworthy levels of piezoelectric voltage and current are discerned, suggesting potential applicability in energizing diverse electronic devices. The generated outputs exhibit the prospect of augmentation and scalability by integrating this fundamental nanostructure layer with additional layers of the same or diverse types. Capitalizing on its attributes of cost-effectiveness, straightforward manufacturing, robust responsiveness, high stability, and repeatability, the crafted nanogenerator emerges as a promising contender for proficient electric energy generation. The amelioration of such electronic systems could culminate in their deployment within the piezoelectric energy harvesting sector (Gil et al., 2013; Raghavendran, Umapathy, & Karlmarx, 2018), thus contributing to the collective endeavor of energy preservation. This study showcases an approach to the synthesis of zinc oxide (ZnO) nanorods, a fundamental component in piezoelectric nanogenerators (NGs). By employing a carefully optimized Chemical Bath Deposition technique, we have achieved the production of well-aligned and high-quality ZnO nanorods. Notably, our research showcases a remarkable fourfold enhancement in the average output voltage. These findings highlight the originality and practicality of our work, positioning it as a valuable resource for advancing energy harvesting capabilities in piezoelectric NGs and contributing to sustainable power generation from mechanical sources.

2. EXPERIMENTAL DETAILS

2.1 Materials

All chemicals and solvents were used in their original state without undergoing any additional purification. Zinc acetate ($ZnC_4H_6O_4$) [99.9% purity], zinc nitrate ($Zn(NO_3)_2$) [98% purity], sodium hydroxide (NaOH), and hexamethylenetetramine[99+% purity] were obtained from Aldrich, while acetone (CH_3COCH_3)[Min 99%] and ethylene glycol ($C_2H_6O_2$) [≥ 99.0 %] were procured from a Sober Life Co.. Other materials used were sourced from commercial suppliers.

2.2 Device

fabrication: Initially, the glass substrate samples were undergone a thorough cleaning process (acetone and ethanol). After that, ethanol and zinc acetate powder were carefully mixed to create a growth solution by adjusting the concentrations of sodium hydroxide (NaOH) and deionized water (DI water), it was possible to precisely control the solution's PH.

To ensure the uniformity of the prepared solution, a magnetic stirrer was used for one hour at room temperature.

Glass as a substrate was applied by spraying (spraying works by first subjecting the source material to a high degree of heat to achieve a molten state. The molten material is then atomized into small particles and sprayed outwards onto a surface), A piece of glass is brought, placed on the heater after cleaning it, and sprayed on it several times with a sprayer until it is completely covered (Измайлов et al., 2017).

and then subjected to a two-hour drying process in an oven set at 300 ^{0}C. Another solution was created by mixing zinc nitrate with DI water, and hexamethylenetetramine was added to the mixture (Sugunan, Warad, Boman, & Dutta, 2006). This new solution was also stirred using a magnetic stirrer for an hour at room temperature.

The solution from the seed layer was carefully combined with the solution from the growth. The flask was sealed, and the mixture was placed inside an oven for 5 hours at a controlled temperature of 95 ^{o}C(Alolyan & Simos, 2015). After the thermal treatment, the flask was removed from the oven and immersed in DI water. Subsequently, it underwent an additional two-hour drying phase in an oven at 300 ^{o}C(Price & NJ, 1971). The resulting product then underwent further processing to convert it into a nanodevice. The fabricated ZnO nanorods electrode is then covered by a conductive PDOT: PSS (prepared from Sigm-Aldrich, the product of Belgium) polymer layer using a spin coating technique, and a layer of PDMS polymer is added to the top of them, forming a nanogenerator (Fig. 1).

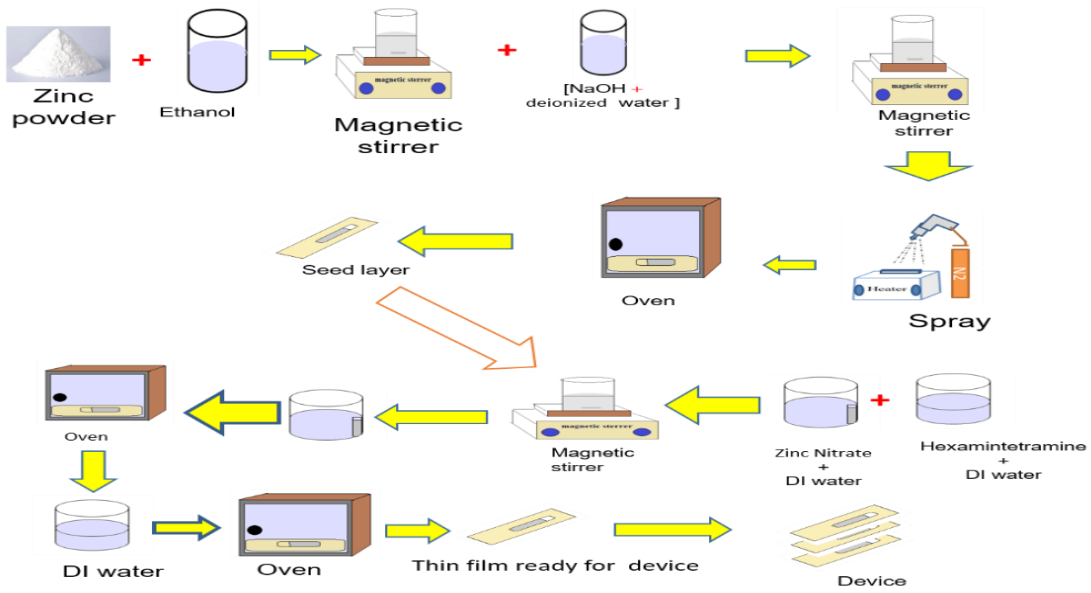

Figure 1: Schematic representation of nanogenerator device fabrication

Producing slim layers from liquid zinc oxide involves employing a technique known as spray coating on glass substrates equipped with heaters. In this method, a liquid mixture containing dispersed, micro-sized particles of the desired nanomaterial is loaded into a spray coating device. The device emits a fine mist of the mixture onto the glass substrate positioned on top of a heater. The heater maintains a consistent temperature, causing the solvent to evaporate and promoting the formation of a uniform slim layer. As the mist settles on the heated substrate, the solvent dissipates, allowing the micro-sized particles to come together and create a slim layer. The integration of the spray coating device, the heater, and the glass substrate enables precise and efficient application of the nanomaterials, resulting in slim layers with tailored characteristics. This illustration depicts the sample manufacturing process, as indicated in Figure 2.

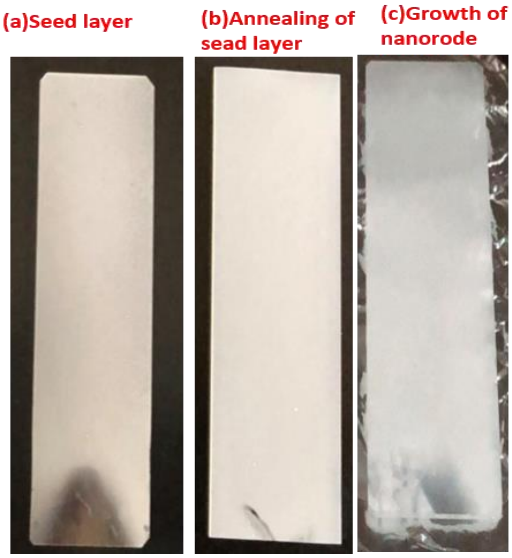

Figure 2: real photos of the ZnO nanorod layer preparation stages (a)seed layer, (b)after annealing, and (c)growth seed layer

2.3 Characterization:

The obtained thin films were undergone characterization using various techniques. The morphology of the samples was analyzed using a scanning electron microscope (SEM – Quanta 450). The atomic composition of the elements was confirmed by energy-dispersive X-ray (EDX) spectroscopy, performed at SEM. Furthermore, the quantum properties of the thin films were evaluated at room temperature through X-ray diffraction (XRD) (reference code. 98-005-7478) measurements using a PAN X' Pert PRO analyzer (Cu Kα = 1.5406 Å), which allowed the examination of possible phase and crystallinity, along with radiograph recording spectrophotometry. The absorption spectra of the 2D nanoscale multi-material thin films prepared on a glass substrate were studied using visible ultraviolet light (Shimadzu UV-160A). The electrical properties of the fabricated nanogenerator were carried out using the Keithley 2450 source meter equipped with a two-probe technique.

3. RESULTS AND DISCUSSION

To assess the morphology characteristics of the fabricated sleek coatings, it utilizes scanning electron microscopy (SEM). SEM images are taken at various magnification levels, spanning from the lowest to the highest resolution. At lower magnifications, SEM offers a wide view of the specimen's surface, revealing the overall morphology of the ZnO nanorod thin film. The first study by Yuan et al. 2020 investigated the leaf epidermis morphology of various plant species using different specimen preparation methods. They found that the resolution of images of conventional SEM leaf samples was generally higher than those obtained using a Coolstage, but local collapse and shrinkage were observed in leaves with high water content using the conventional method (Yuan et al., 2020). The ZnO nanorods obtained exhibit a notably slender shape, with an average length of 400 nm. These images uncover the presence of creases, folds, or strata misalignments, which are effectively concealed within the film after the growth stage. Figure (3f) reveals the uniformity of the film coverage and growth of ZnO nanorods.

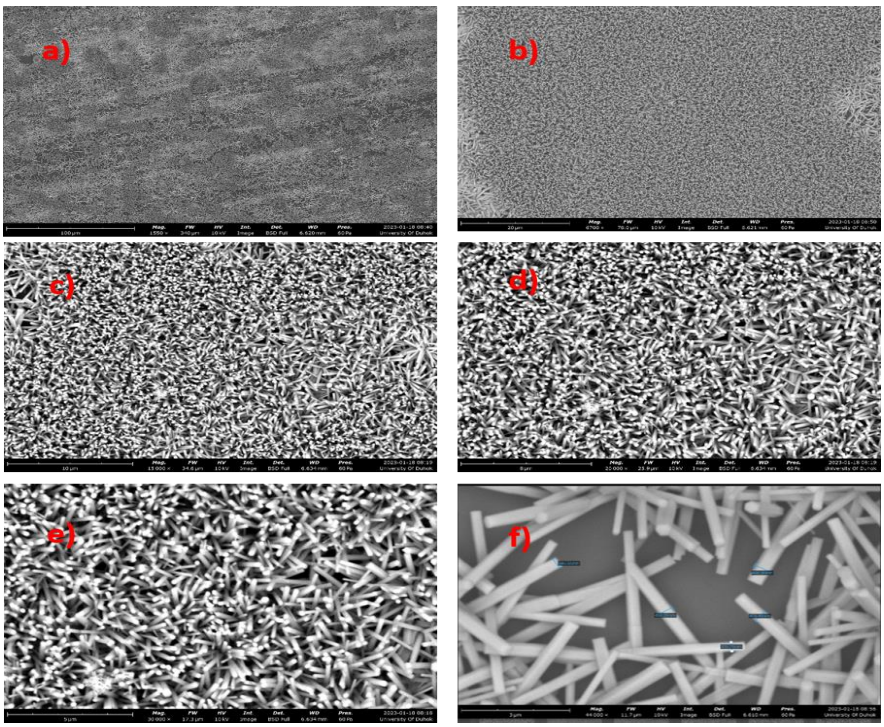

Figure 3: SEM images of ZnO nanorods thin films

XRD patterns of thin films containing ZnO nanorods usually show different diffraction peaks, each of which corresponds to a different crystallographic plane in the ZnO crystal structure (fig.5). Parwani et al. synthesized Zn-doped ZnO samples and analyzed their structure using XRD. The changes observed in crystallinity and particle size were due to Zn dopin(Parwani, Dubey, Dixit, & Kaurav, 2019). These characteristic peaks are typically detected at specific 2θ angles, offering valuable insights into the structural attributes of the film. Nobaly, a clear peak can be Seen at about 2θ ≈ 34.4°, which is the (002) crystallographic plane. This suggests that the ZnO nanorods are most likely to be aligned along the c-axis. Another robust peak at roughly 2θ ≈ 36.1° corresponds to the (101) crystallographic plane, indicating a highly crystalline hexagonal structure. Additionally, there is a discernible peak near 2θ ≈ 62.8°, associated with the (102) crystallographic plane, further corroborating the hexagonal nature of the ZnO nanorods. It is important to note that the precise positions and intensities of these peaks can vary due to factors like growth conditions, nanorod size, and potential strains or defects in the thin film, emphasizing the necessity of comprehensive XRD characterization.

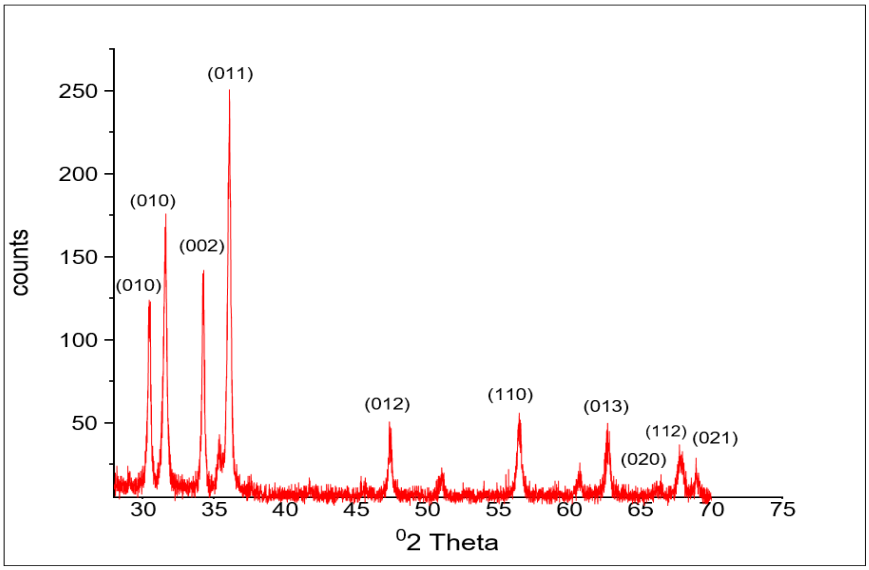

Figure. 4: XRD pattern of the deposited thin film. Diffraction peaks are indexed from the zinc oxide phases

According to the elemental proportions extracted from the EDX analysis presented in Figure 6, the fabricated thin film contains a significant proportion of zinc, constituting approximately 32.10% of its atomic composition. Notably, there is also a substantial concentration of oxygen, making up 53.39% of the atomic composition, while silicon and calcium account for 10.34% and 4.15% respectively. It is conceivable that the sample may have been exposed to air either during its production or during the analytical process, resulting in surface oxidation, and the silver appears because the sample was not pure, a study by Hemant K. Verma et al. synthesized ZnO nanomaterials using sol-gel techniques and found that they exhibited higher photocatalytic activity field (SHUKLA, Sharma, & Maurya, 2022).

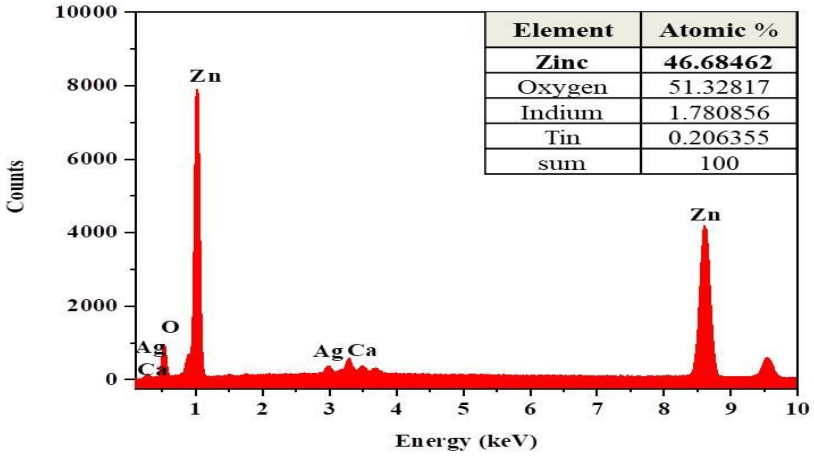

Figure5: EDX analysis of the Zinc oxide. The inset is the elemental atomic percentage.

Further investigation of the optical properties of the prepared ZnO nanorods was conducted. A ZnO thin film has the unique ability to selectively capture specific light wavelengths, resulting in a decrease in the intensity of light that passes through it. Primarily, ZnO demonstrates a penchant for absorbing light in the ultraviolet (UV) spectrum, owing to its distinctive energy structure (see Fig. 7). This passage delves into the concept of zinc oxide's influence on light transmission in glass, which pertains to the degree of light that traverses the material. In situations where zinc oxide does not strongly absorb light, the passage of light remains significantly robust. Glasses incorporating zinc oxide can exhibit admirable transparency within the visible spectrum, typically spanning wavelengths from 300 to 400 nm. The level of transparency is contingent upon the quantity of zinc oxide and other constituents in the glass. The extent of this light capture depends on the energy states occupied by electrons within the ZnO crystal lattice, in conjunction with the energy carried by incoming photons (Balakrishna et al., 2018; Saharan, 2022).

The concentration of zinc oxide within the glass composition significantly affects the characteristics of light absorption and transmission (Tab, Abderrahmane, Bakha, Hamzaoui, & Zerdali, 2019). Reduced amounts of ZnO in the glass tend to enhance clarity across a broader range of wavelengths. Conversely, higher concentrations may lead to increased absorption, especially in the UV spectrum (see Fig. 7a).

The bandgap energy (Eg) of the prepared thin films was determined by analyzing their transmittance curves. For this analysis, the photon energy (hv) against the square of the product of the absorption coefficients of the photon energy $(\alpha hv)^2$ was plotted. The Eg values were obtained by extrapolating the linear part of the (αhv)1/2-hν curve to the corresponding horizontal photon energy axis, applying Tauc's law (Hadi, Shur, & O'Leary, 2014) (see Fig. 7.b).
The energy gap value for multilayer zinc oxide thin films was estimated to be 3.5 eV, corresponding to the transition from the valence band to the conduction band. A similar energy gap is anticipated to emerge in multiple layers of zinc oxide, and the magnitude of the gap is contingent upon the number of layers (Haq, Ahmed, & Goumri-Said, 2014).

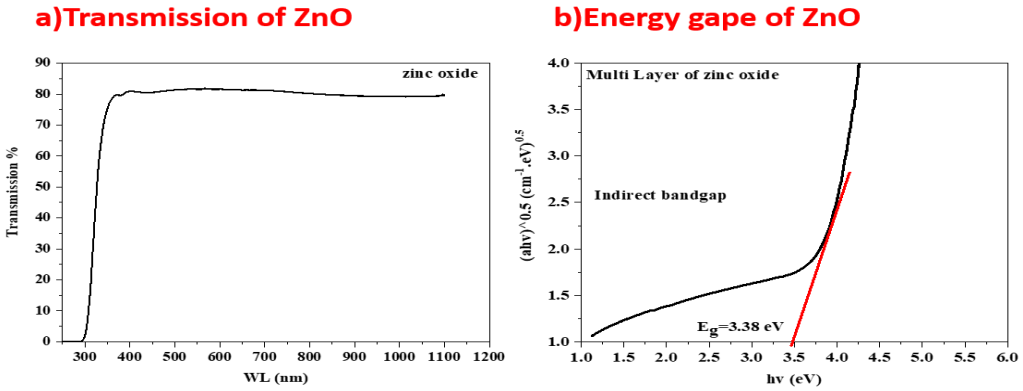

Figure 6: a) Transmission of zinc oxide and b) Energy gap of zinc oxide

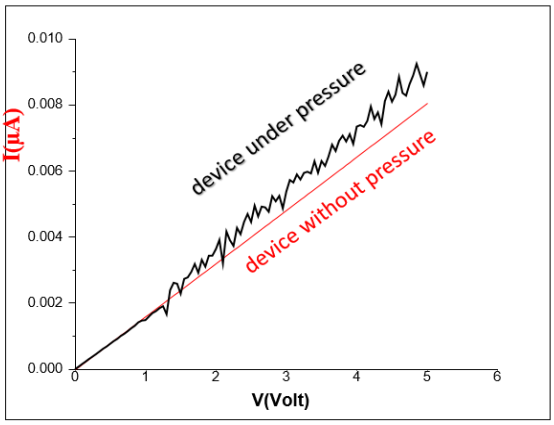

Figure.7: The relationship of current and voltage with and without pressure of the fabricated nanogenerator

4. CONCLUSION

In conclusion, this study has presented a significant advancement in the synthesis and application of ZnO nanorods in the realm of piezoelectric nanogenerators (NGs). The efficient and scalable synthesis method yielded well-aligned and high-quality ZnO nanorods, demonstrating remarkable piezoelectric properties with heightened sensitivity to mechanical deformation. These findings not only underscore the potential of ZnO nanorods as ideal candidates for NG applications but also emphasize the crucial role of the proposed synthesis method in enhancing their performance.

Enhancing the nanogenerator's operational capabilities can be achieved by optimizing the process of electrical charge induction through the incorporation of a consistently pre-charged electrode material. These approaches are geared towards augmenting the nanogenerator's overall output efficiency and performance, rendering it a more viable and efficient solution for energy harvesting applications. The piezoelectric effect of the prepared ZnO nanoroads used within the fabricated nanogenerator be seen when a mechanical pressure is supplied to the device, at which point a tremendous increase in the amount of output current can be seen.

The influence of thermal annealing on ZnO nanopowders was studied, with annealing at 500°C resulting in an average output voltage of 1.95 V, a fourfold increase compared to as-deposited nanopowders [4]. This study has indicated the potential of ZnO-based nanogenerators for harvesting mechanical energy and self-powered electronic applications (Ariffin et al., 2023).

5. ACKNOWLEDGMENTS

This research was sponsored by the Department of Physics, College of Science, Duhok University.

6. REFERENCES

Alolyan, I., & Simos, T. (2015). Efficient low computational cost hybrid explicit four-step method with vanished phase-lag and its first, second, third and fourth derivatives for the numerical integration of the Schrödinger equation. Journal of Mathematical Chemistry, 53, 1808-1834.

Amna, T. (2018). Shape-controlled synthesis of three-dimensional zinc oxide nanoflowers for disinfection of food pathogens. Zeitschrift für Naturforschung C, 73(7-8), 297-301.

Ariffin, N. K., Mamat, M., Kamaruzaman, D., Abdullah, M., Parimon, N., Yaakob, M., . . . Mohamed, A. (2023). Metal-doped zinc oxide nanostructures for nanogenerator applications: A review. Materials Today: Proceedings, 75, 51-57.

Aziz, N. S. A., Nishiyama, T., Rusli, N. I., Mahmood, M. R., Yasui, K., & Hashim, A. M. (2014). Seedless growth of zinc oxide flower-shaped structures on multilayer graphene by electrochemical deposition. Nanoscale research letters, 9, 1-9.

Balakrishna, A., Pathak, T. K., Coetsee-Hugo, E., Kumar, V., Kroon, R., Ntwaeaborwa, O., & Swart, H. (2018). Synthesis, structure and optical studies of ZnO: Eu3+, Er3+, Yb3+ thin films: Enhanced up-conversion emission. Colloids and Surfaces A: Physicochemical and Engineering Aspects, 540, 123-135.

Fan, J., Li, T., & Heng, H. (2014). Hydrothermal growth and optical properties of ZnO nanoflowers. Materials Research Express, 1(4), 045024.

Fan, J., Li, T., & Heng, H. (2016). Hydrothermal growth of ZnO nanoflowers and their photocatalyst application. Bulletin of Materials Science, 39, 19-26.

Fan, Z., & Lu, J. G. (2005). Zinc oxide nanostructures: synthesis and properties. Journal of nanoscience and nanotechnology, 5(10), 1561-1573.

Gil, M., Manzaneque, T., Hernando-García, J., Ababneh, A., Seidel, H., & Sánchez-Rojas, J. L. (2013). Multimodal characterisation of high-Q piezoelectric micro-tuning forks. IET Circuits, Devices & Systems, 7(6), 361-367.

Hadi, W. A., Shur, M. S., & O'Leary, S. K. (2014). Steady-state and transient electron transport within the wide energy gap compound semiconductors gallium nitride and zinc oxide: an updated and critical review. Journal of Materials Science: Materials in Electronics, 25, 4675-4713.

Haq, B. U., Ahmed, R., & Goumri-Said, S. (2014). DFT characterization of cadmium doped zinc oxide for photovoltaic and solar cell applications. Solar energy materials and solar cells, 130, 6-14.

Ji, J., Yang, C., Shan, Y., Sun, M., Cui, X., Xu, L., . . . Luo, D. (2023). Research Trends of Piezoelectric Nanomaterials in Biomedical Engineering. Advanced NanoBiomed Research, 3(1), 2200088.

Kaur, J., Singh, H., & Singh, A. (2020). Fabrication and investigation of zinc oxide nanoflowers-based piezoelectric nanogenerator. IET Circuits, Devices & Systems, 14(4), 477-483.

Kołodziejczak-Radzimska, A., & Jesionowski, T. (2014). Zinc oxide—from synthesis to application: a review. Materials, 7(4), 2833-2881.

Krishnakumar, T., Jayaprakash, R., Pinna, N., Singh, V., Mehta, B., & Phani, A. (2009). Microwave-assisted synthesis and characterization of flower shaped zinc oxide nanostructures. Materials Letters, 63(2), 242-245.

Krithika, G., Saraswathy, R., Muralidhar, M., Thulasi, D., Lalitha, N., Kumararaja, P., . . . Jayavel, R. (2017). Zinc oxide nanoparticles—Synthesis, characterization and antibacterial activity. Journal of nanoscience and nanotechnology, 17(8), 5209-5216.

Kumar, K. M., Mandal, B. K., Naidu, E. A., Sinha, M., Kumar, K. S., & Reddy, P. S. (2013). Synthesis and characterisation of flower shaped zinc oxide nanostructures and its antimicrobial activity. Spectrochimica Acta Part A: Molecular and Biomolecular Spectroscopy, 104, 171-174.

Mavundla, S., Malgas, G., Motaung, D., & Iwuoha, E. (2012). Synthesis of flower-like zinc oxide and polyaniline with

worm-like morphology and their applications in hybrid solar cells. Crystal Research and Technology, 47(5), 553-560.

Öztürk, S., Kılınç, N., Taşaltın, N., & Öztürk, Z. Z. (2012). Fabrication of ZnO nanowires and nanorods. Physica E: Low-Dimensional Systems and Nanostructures, 44(6), 1062-1065.

Paino, I. M., J. Gonçalves, F., Souza, F. L., & Zucolotto, V. (2016). Zinc oxide flower-like nanostructures that exhibit enhanced toxicology effects in cancer cells. ACS Applied Materials & Interfaces, 8(48), 32699-32705.

Parwani, S., Dubey, P., Dixit, R., & Kaurav, N. (2019). XRD and FTIR studies of zinc doped nickel oxide compounds. Paper presented at the AIP Conference Proceedings.

Price, A. E., & NJ, C. R. C. S. (1971). PBI Tow Manufacturing Methods.

Raghavendran, S., Umapathy, M., & Karlmarx, L. R. (2018). Supercapacitor charging from piezoelectric energy harvesters using multi-input buck–boost converter. IET Circuits, Devices & Systems, 12(6), 746-752.

Rezaei, R., Foroughi, M. M., Beitollahi, H., Tajik, S., & Jahani, S. (2019). Synthesis of lanthanium-doped ZnO nanoflowers: Supported on graphite screen printed electrode for selective and sensitive detection of hydrochlorothiazide. International Journal of Electrochemical Science, 14(2), 2038-2048.

Rihtnesberg, D. B., Almqvist, S., Wang, Q., Sugunan, A., Yang, X., Toprak, M. S., . . . Göthelid, M. (2011). ZnO nanorods/nanoflowers and their applications. Paper presented at the The 4th IEEE International NanoElectronics Conference.

Saharan, C. (2022). Enhanced Visible Light Transmittance and Phase Transition in ZnO/VO2/AL2O3 Bilayer Thin Film for Energy Efficient Smart Windows. Paper presented at the Electrochemical Society Meeting Abstracts 242.

Shang, T. M., Sun, J. H., Zhou, Q. F., & Guan, M. Y. (2007). Controlled synthesis of various morphologies of nanostructured zinc oxide: flower, nanoplate, and urchin. Crystal Research and Technology: Journal of Experimental and Industrial Crystallography, 42(10), 1002-1006.

Sharma, S., Dalal, V. S., & Mahajan, V. (2016). Synthesis of Zinc oxide nano flower for photovoltaic applications. Materials Today: Proceedings, 3(6), 1359-1362.

Shinde, S., Shinde, P., Bhosale, C., & Rajpure, K. (2011). Zinc oxide mediated heterogeneous photocatalytic degradation of organic species under solar radiation. Journal of Photochemistry and Photobiology B: Biology, 104(3), 425-433.

SHUKLA, D., Sharma, A. K., & Maurya, A. (2022). Studies on performance and emission analysis of a CI engine using zinc oxide nanoparticles with biodiesel.

Subramani, K., & Sathish, M. (2019). Facile synthesis of ZnO nanoflowers/reduced graphene oxide nanocomposite using zinc hexacyanoferrate for supercapacitor applications. Materials Letters, 236, 424-427.

Sugunan, A., Warad, H. C., Boman, M., & Dutta, J. (2006). Zinc oxide nanowires in chemical bath on seeded substrates: role of hexamine. Journal of Sol-Gel Science and Technology, 39, 49-56.

Sun, Y., Zheng, Y., Wang, R., Fan, J., & Liu, Y. (2021). Direct-current piezoelectric nanogenerator based on two-layer zinc oxide nanorod arrays with equal c-axis orientation for energy harvesting. Chemical engineering journal, 426, 131262.

Tab, A., Abderrahmane, A., Bakha, Y., Hamzaoui, S., & Zerdali, M. (2019). Investigation on the optical transmission in UV range of sol-gel spin coated zinc oxide nanofilms deposited on glass. Optik, 194, 163073.

Tajik, S., Beitollahi, H., & Aflatoonian, M. R. (2019). A novel dopamine electrochemical sensor based on La3+/ZnO nanoflower modified graphite screen printed electrode. Journal of Electrochemical Science and Engineering, 9(3), 187-195.

Umetsu, M., Mizuta, M., Tsumoto, K., Ohara, S., Takami, S., Watanabe, H., . . . Adschiri, T. (2005). Bioassisted room-temperature immobilization and mineralization of zinc oxide—The structural ordering of ZnO nanoparticles into a flower-type morphology. Advanced Materials, 17(21), 2571-2575.

Wahab, R., Hwang, I., Kim, Y.-S., & Shin, H.-S. (2011). Photocatalytic activity of zinc oxide micro-flowers synthesized via solution method. Chemical engineering journal, 168(1), 359-366.

Wang, Z. L. (2004). Zinc oxide nanostructures: growth, properties and applications. Journal of physics: condensed matter, 16(25), R829.

Xie, L., Xu, Y., & Cao, X. (2013). Hydrogen peroxide biosensor based on hemoglobin immobilized at graphene, flower-like zinc oxide, and gold nanoparticles nanocomposite modified glassy carbon electrode. Colloids and Surfaces B: Biointerfaces, 107, 245-250.

Yang, R.-T., Yu, H.-Y., Song, M.-L., Zhou, Y.-W., & Yao, J.-M. (2016). Flower-like zinc oxide nanorod clusters grown on spherical cellulose nanocrystals via simple chemical precipitation method. Cellulose, 23, 1871-1884.

Yuan, J., Wang, X., Zhou, H., Li, Y., Zhang, J., Yu, S., . . . Liu, L. (2020). Comparison of sample preparation techniques for inspection of leaf epidermises using light microscopy and scanning electronic microscopy. Frontiers in Plant Science, 11, 133.

Измайлов, А. Ю., Голубкович, А. В., Павлов, С. А., Павлова, И. Ю., Потапов, А. В., Марин, Р. А., & Дадыко, А. Н. (2017). Способ осциллирующей сушки зерна.